



Correction of Fluorescent Probe Degradation in Biodistribution Studies

Boklund, Tobias Idor ; Fromberg, Laurits ; Henriksen, Christian; Jüttner, Benjamin; Olesen, Peder Jørgensgaard; Plesner, Andreas ; Scheel, Kenneth

Link to article, DOI:
[10.33774/miir-2022-cvrmf](https://doi.org/10.33774/miir-2022-cvrmf)

Publication date:
2022

Document Version
Early version, also known as pre-print

[Link back to DTU Orbit](#)

Citation (APA):
Boklund, T. I., Fromberg, L., Henriksen, C., Jüttner, B., Olesen, P. J., Plesner, A., & Scheel, K. (2022). *Correction of Fluorescent Probe Degradation in Biodistribution Studies*. Cambridge University Press. Mathematics in Industry <https://doi.org/10.33774/miir-2022-cvrmf>

General rights

Copyright and moral rights for the publications made accessible in the public portal are retained by the authors and/or other copyright owners and it is a condition of accessing publications that users recognise and abide by the legal requirements associated with these rights.

- Users may download and print one copy of any publication from the public portal for the purpose of private study or research.
- You may not further distribute the material or use it for any profit-making activity or commercial gain
- You may freely distribute the URL identifying the publication in the public portal

If you believe that this document breaches copyright please contact us providing details, and we will remove access to the work immediately and investigate your claim.

Correction of Fluorescent Probe Degradation in Biodistribution Studies

TOBIAS IDOR BOKLUND¹,
LAURITS FROMBERG¹, CHRISTIAN HENRIKSEN¹†, BENJAMIN JÜTTNER¹, PEDER
JØRGENSGAARD OLESEN¹, ANDREAS PLESNER¹ and KENNETH SCHEEL¹

¹ *Technical University of Denmark, Kongens Lyngby, Denmark*

(Communicated to MIIR on February 18, 2022)

Study Group: 160th European Study Group With Industry (ESGI), August 16-20 2021

Communicated by: Poul G. Hjorth

Industrial Partner: Gubra

Presenter: Casper G. Salinas

Team Members: T. I. Boklund, L. Fromberg, C. Henriksen, B. Jüttner, P. J. Olesen, A. Plesner, K. Scheel,

Industrial Sector: Biomedical/Healthcare

Tools: Statistical Modeling, Maximum Likelihood Estimation, Mixed-Effects Models

Key Words: Fluorescence Microscopy, Tissue degradation, Photobleaching

MSC2020 Codes: 62J02, 62P10

† Corresponding author: chrh@dtu.dk

Summary

Fluorescence microscopy can be used for evaluating the distribution of medical compounds in animal tissue. Fluorescence intensity decays in time and due to scanning, but correcting for this can improve accuracy. We present a mixed-effects model for fluorescence microscopy intensity reconstruction. Model parameters are estimated via maximum likelihood estimation, taking into account biological variability between animals and measurement uncertainty. The initial fluorescence intensity is reconstructed by decay correction.

The model is tested using different data sets. When estimating initial intensities from intensities measured on samples subjected to chemical degradation, decay rate estimates are found to be robust against variation in the ratio of measurement-induced variance to biological variance. Photobleaching rates are found to have only modest significance.

A synthetic data set consistent with previously determined parameters is generated, and a forward model is applied; the maximum likelihood estimates accurately recover the parameters, demonstrating the consistency of the model.

1 Introduction

In vivo distribution studies aim to quantify how a given compound, e.g. medication, is distributed in various types of tissue. A method to measure the compound *in vitro* is fluorescence microscopy. Here a fluorescent label, or fluorophore, is conjugated to the compound, and activated by laser excitation during microscopy. Activation causes a delayed emission of light at a particular wavelength from the fluorophore. Measuring this light facilitates mapping of the distribution of the fluorophore, and thus of the compound of interest to which the fluorophore is conjugated.

The fluorescent labels chemically degrade over time, and the microscopy process additionally degrades them through photobleaching. This may introduce large variation which interferes with the interpretation of the biological variation between samples.

The goal of the present work is to model both modes of degradation such that a correction can be applied to measured intensities, yielding estimates of what the intensities would be in the absence of degradation.

The microscope captures two different sources of fluorescence, the *autofluorescence channel* and the *specific channel*. The former registers wavelengths outside the fluorescence band of the fluorescent label, where the spectrum is dominated by natural fluorescence from the tissue. This signal is independent of the medication given to the subject. The latter channel captures the spectral band where the fluorescent signal emitted by the fluorescent label distributed in the tissue dominates. The light intensity in both channels is subject to degradation.

2 Data

Data set 1 (see Figure 1) displays the intensity¹ of the specific channel in a location of the microscope image where the fluorescent intensity is highest. This is taken for six different groups (batches) of mice, each consisting of five or six individual mice. Tissue from each mouse was scanned (and thereby photobleached) exactly once. The medical compound varies among batches, and the time, t_i , of the microscopy event (where $t = 0$ is the time of sample creation) generally varies among the mice.

Group 1 of this data set is a control group, and the mice in this group have had no fluorescent substance injected.

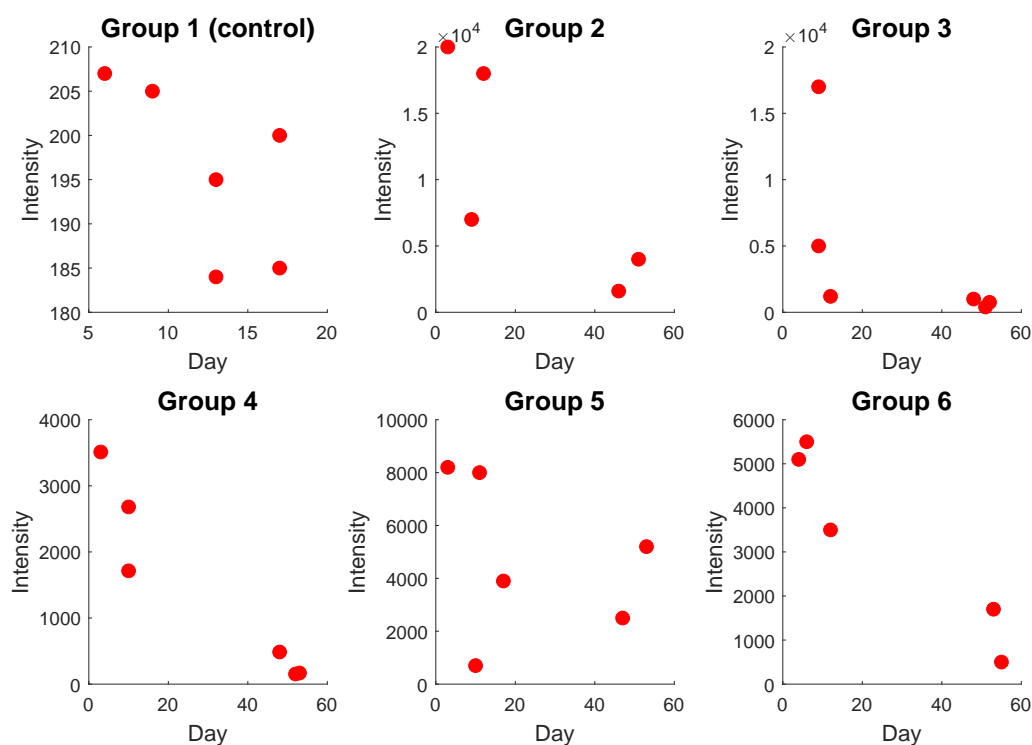


Figure 1. Data set 1. Horizontal axes are number of days in storage before imaging, vertical axes are the maximum fluorescence intensity in each image.

Data set 2 (see Figure 2) also contains the intensity of the specific channel in a location of the microscope image where the fluorescence intensity is highest. Here, however, the intensities are given for only two different mice. These have been injected with compounds labeled with the fluorophores Lectin and Cy5, respectively. Each sample was then imaged (and photobleached) 300 times. Each imaging lasts approximately five seconds, and the time between scans is approximately 1 second². Thus, the total time between the first and last scan is approximately half an hour.

¹ considered a dimensionless quantity throughout this work.

² Casper G. Salinas, Gubra; private communication.

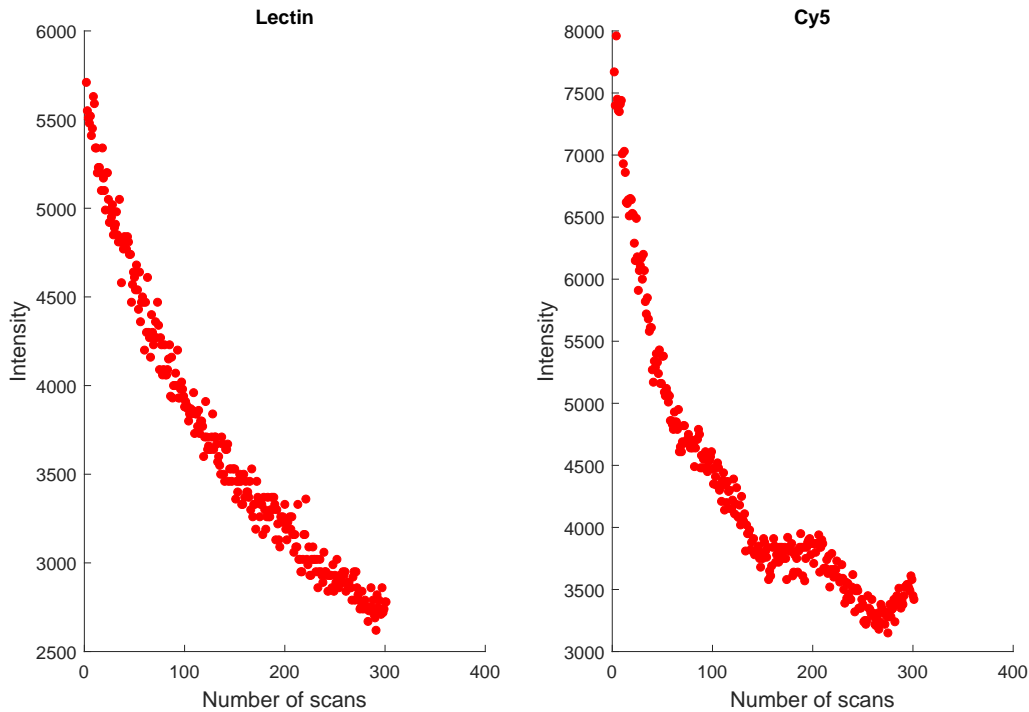


Figure 2. Data set 2. Horizontal axes are number of scans (photobleachings), vertical axes are the maximum fluorescence intensity in each image.

Lastly, in the absence of data sets for tissue samples scanned more than once over an extended period of time, and thus being subject to both chemical degradation and photobleaching, we generated such a data set synthetically, as shown in Figure 3. This data set is similar to data set 1, except that the generated data set contains intensities from numerous tissue samples that have been scanned more than once. The process behind the generation of this data is explained in Section 3.4.

3 Models

3.1 Simple Exponential Degradation Model

A newly acquired sample of animal tissue containing a fluorescence-labeled compound may be stored for some time, during which the fluorescent label will be exposed to chemical degradation. Each fluorescence scan imparts further degradation through photobleaching.

A deterministic forward model which describes both the chemical degradation and the photobleaching is needed to analyze the problem, and a corresponding backward model can then be used to reconstruct the theoretical fluorescence intensity at time zero from an actual intensity measured at a later time.

To make the simplest possible model that can account for chemical decay and photobleaching, we assume the following throughout this work:

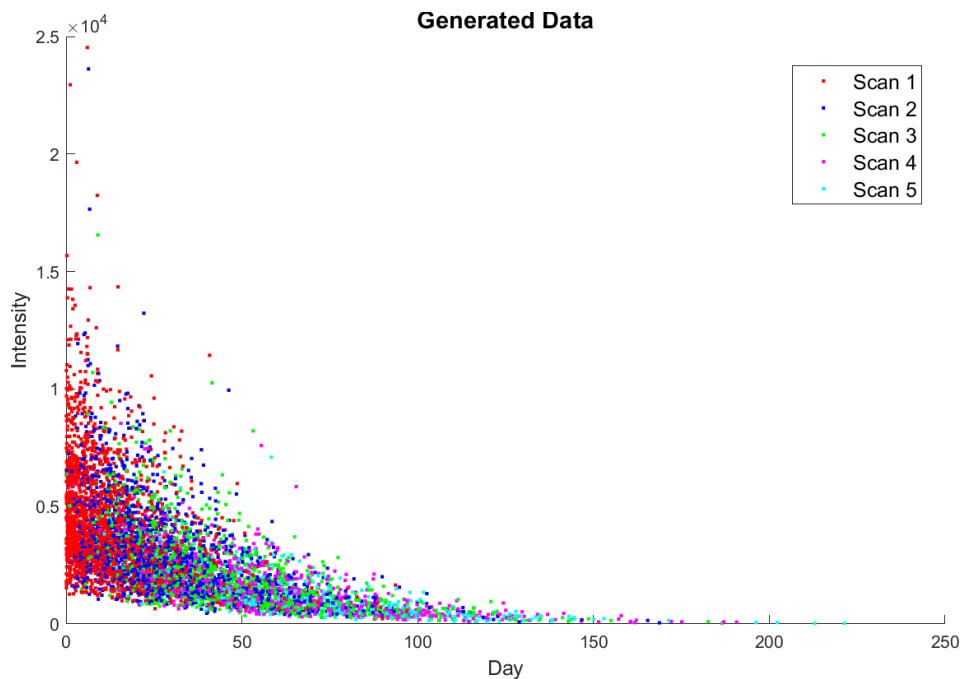


Figure 3. Synthetic data set. Horizontal axis is number of days in storage, vertical axis is the maximum fluorescence intensity in each image. Each point corresponds to a photobleaching scan. Some samples have been scanned more than once, as indicated by colors. The connections between scans from the same sample (at different times) are not shown.

- (1) Chemical degradation causes the intensity to exponentially decay with a rate constant, α , which does not vary in time nor among individual animals, but may depend on the specific compound and fluorescent label.
- (2) A fixed fraction, $e^{-\kappa}$ (with $\kappa \geq 0$; this definition will be useful later), of the fluorescent label present at the beginning of each scan remains after the scan, with the fraction $1 - e^{-\kappa}$ being lost to photobleaching. The value of κ may depend on the specific compound and fluorescent label. However, we assume that scanning parameters such as scan time and intensity of the scanning laser do not vary between scans.
- (3) The intensity obtained in a scan is proportional to the amount of labeled compound remaining at the start of the scan.

Due to different uptakes and biochemical differences, the fluorescent intensity, $I(t)$, at time t , will differ between mice (biological variance) and between different medical substances (compound variance). Further variation in the measured intensity is brought about by measurement variance caused by the sensor. In principle, α might also differ between mice. However as stated in assumption (1) this possibility is not considered in this work.

Assumptions (1) and (2) can be summarized in the following basic expression for the intensity at time t for a sample having been exposed to $M = M(t)$ scans:

$$I(t) = I^0 e^{-\alpha t - M\kappa}. \quad (3.1)$$

It follows that the initial intensity can be calculated from the intensity at time t , by the following backward expression:

$$I^0 = I(t) e^{\alpha t + M\kappa}. \quad (3.2)$$

On a side note, assumption (2) represents photobleaching as a discrete event. Photobleaching might actually be modelled using different forms and combinations of exponential decay[2]. If photobleaching is interpreted as a single exponential decay, one could rewrite Equation (3.1) as $I(t) = I^0 e^{-\alpha t - M\beta\tau}$, where β and τ are respectively the decay rate due to photobleaching and the duration of the microscopy event. However, since the latter is (approximately) constant and very short (a sample is only exposed to the laser for ~ 5 s when scanned³) compared to the storage time of a sample (up to 60 days), we choose to simply collapse the two constants β and τ into κ .

Taking the natural logarithm, letting $J(t) = \log(I(t))$ and $J^0 = \log(I^0)$, Equations (3.1) and (3.2) read

$$J(t) = J^0 - \alpha t - M\kappa, \quad (3.3)$$

and

$$J^0 = J(t) + \alpha t + M\kappa, \quad (3.4)$$

respectively. From these two equations it becomes apparent why it is advantageous to work with log-intensities instead of directly with intensities: The effect of degradation (α) and photobleaching (κ) becomes linear if we fix time (t).

In the following, the simple model (3.3) is refined by taking into account the stochastic variance brought about by biological variance and measurement uncertainty.

3.2 A Statistical Model and Maximum Likelihood Estimation of the Parameters

In this subsection, we build a simple statistical model and show how one can estimate the parameters in the model. In a data set like data set 1 in Section 2, where each sample is scanned only once, we can neglect photobleaching. Also, as we shall see in Section 4.2, photobleaching might be a relatively weak effect, so it makes sense to first disregard this effect, which effectively corresponds to setting $\kappa = 0$ in Equation (3.1).

3.2.1 Parameter estimation without photobleaching

In data set 1 each mouse has been scanned exactly once, and we need not take degradation due to photobleaching into account for these mice. Setting $\kappa = 0$ in Equation (3.3) gives

$$J(t) = J^0 - \alpha t. \quad (3.5)$$

³ Casper G. Salinas, Gubra; private communication.

Table 1. List of symbols introduced for maximum likelihood parameter estimation.

Symbol	Explanation
n	Number of mice in the batch.
t_i	Time at which mouse i is scanned, where $i = 1, 2, \dots, n$.
\tilde{J}_i	Measured log-intensity for mouse i at time t_i .
J_i^0	True log-intensity of mouse i at time 0.
\mathcal{J}	Expected log-intensity for the batch at time 0.
ϵ_i	Log-measurement error of scan i .
σ^2	Variance of log-measurement error.
$\sigma_{\mathcal{J}}^2$	Biological variance of (true) J_i^0 within a batch.

Since each batch is treated separately we do not employ a batch index in the following. We let t_i denote the time at which sample i is scanned, and let \tilde{J}_i denote log of the measured intensity.

We take two stochastic effects into account in our model; firstly, that the different samples are distinct, so that the starting intensities cannot be assumed to be equal, and secondly, the measurement error occurring at each scan.

We assume that the log-intensities, J_i^0 , for all mice at $t = 0$ follow a normal distribution with mean \mathcal{J} and variance $\sigma_{\mathcal{J}}^2$, i.e., $J_i^0 \sim \mathcal{N}(\mathcal{J}, \sigma_{\mathcal{J}}^2)$. In other words, we assume that $J_i^0 = \mathcal{J} + u_i$, where $u_i \sim \mathcal{N}(0, \sigma_{\mathcal{J}}^2)$ is the random effect of the sample tissue (the mice) being distinct.

We also assume that the stochastic log-measurement errors follow a normal distribution with mean zero and variance σ^2 , i.e., $\epsilon_i \sim \mathcal{N}(0, \sigma^2)$. Our statistical model is then

$$\tilde{J}_i = J_i(t_i) + \epsilon_i = J_i^0 - \alpha t_i + \epsilon_i = \mathcal{J} - \alpha t_i + u_i + \epsilon_i. \quad (3.6)$$

Finally we assume that the stochastic variables J_i^0 , ϵ_i , $i = 1, \dots, n$ are all independent. Table 1 summarizes the different symbols used.

We now turn to estimating the parameters $\boldsymbol{\theta} := [J_1^0, \dots, J_n^0, \mathcal{J}, \alpha]$. The estimators obtained using the maximum likelihood method are the parameter values that maximize the likelihood function \mathcal{L} , i.e., the joint probability density function (PDF) of the stochastic variables, J_i^0 and ϵ_i , for $i = 1, \dots, n$. Since we have assumed the latter to be independent, the joint PDF can be computed as the product of the PDFs for the individual stochastic variables:

$$\mathcal{L} = \text{PDF}(\epsilon_1, \dots, \epsilon_n, J_1^0, \dots, J_n^0, \alpha, \mathcal{J}) = \prod_{i=1}^n \text{PDF}(J_i^0) \cdot \text{PDF}(\epsilon_i), \quad (3.7)$$

$$\text{PDF}(J_i^0) = \frac{1}{\sqrt{2\pi\sigma_{\mathcal{J}}^2}} \exp\left(-\frac{(J_i^0 - \mathcal{J})^2}{2\sigma_{\mathcal{J}}^2}\right), \quad (3.8)$$

$$\text{PDF}(\epsilon_i) = \frac{1}{\sqrt{2\pi\sigma^2}} \exp\left(-\frac{(J_i^0 - \alpha t_i - \tilde{J}_i)^2}{2\sigma^2}\right). \quad (3.9)$$

This yields an expression for the likelihood function \mathcal{L} where normalization factors have

been omitted as they do not alter the solution to the subsequent optimization problem:

$$\mathcal{L} = \prod_{i=1}^n \exp\left(-\frac{(J_i^0 - \mathcal{J})^2}{2\sigma_{\mathcal{J}}^2}\right) \exp\left(-\frac{(J_i^0 - \alpha t_i - \tilde{J}_i)^2}{2\sigma^2}\right). \quad (3.10)$$

We take the negative logarithm of the likelihood function to turn the maximization problem into a simpler minimization problem:

$$-\log \mathcal{L} = \frac{1}{2} \sum_{i=1}^n \left(\frac{(J_i^0 - \mathcal{J})^2}{\sigma_{\mathcal{J}}^2} + \frac{(J_i^0 - \alpha t_i - \tilde{J}_i)^2}{\sigma^2} \right). \quad (3.11)$$

We define $\rho^2 := \frac{\sigma^2}{\sigma_{\mathcal{J}}^2}$ and multiply the expression by σ^2 (this does not alter the solution to the optimization problem) to discard the denominator in the second term, such that ρ^2 acts as a weight in the optimization problem. This yields the following minimization problem for estimating the parameters:

$$\hat{\theta} = \arg \min_{\theta} \frac{1}{2} \sum_{i=1}^n \left(\rho^2 (J_i^0 - \mathcal{J})^2 + (J_i^0 - \alpha t_i - \tilde{J}_i)^2 \right), \quad (3.12)$$

where $\hat{\theta}$ denotes the vector of maximum likelihood estimates of the parameters. This is an unconstrained least squares problem which can be solved by differentiating and solving a linear system of equations, or simply by calling a minimization routine such as `fminunc` in MATLAB. Introducing the constraint $\alpha > 0$, we get a constrained optimization problem that can be solved with routines such as `fmincon` in MATLAB.

The parameter ρ^2 represents the ratio of the variance due to measurement to the biological variance and is thus a measure of the relative importance of these sources of variation among data points. While ρ^2 is not known *a priori*, we can try different educated guesses to adjust the weighing of each term in the optimization.

We need to supply the measured log-transformed intensities, \tilde{J}_i , measurement times, t_i , and a value for ρ^2 . From this we acquire the maximum likelihood estimates for the initial log-intensity, J_i^0 , for each mouse i , the mean log-intensity, \mathcal{J} , and the chemical degradation rate, α . These parameter values can then be used to backtrack and plot the chemical degradation estimates as a function of time. These estimates ought to be applied separately for each group of mice tested on different labeled compounds, or for different batches of samples.

3.2.2 Parameter estimation with photobleaching

Assuming that each sample can be scanned more than once during its storage time, we denote the number of times sample i has been scanned by the variable $\mu(i)$. If sample i has been scanned three times ($\mu(i) = 3$), we will have three measurements, \tilde{J}_{i1} , \tilde{J}_{i2} , and \tilde{J}_{i3} at times t_{i1} , t_{i2} , and t_{i3} , and similarly for other values of $\mu(i)$.

In data set 1, each sample was scanned only once ($\mu(i) = 1$, for all $1 \leq i \leq n$). This led us to consider a method for generating an artificial data set with $\mu(i) \geq 1$, which

statistically resembles the original data (see Section 3.4). A model which takes both chemical degradation and photobleaching into account has an additional exponential factor as follows:

$$I_i(t_{ij}) = I_i^0 e^{-\alpha t_{ij}} (e^{-\kappa})^{j-1}. \quad (3.13)$$

We have chosen the convention $j - 1$ in the exponent of the photobleaching term to signify that the photobleaching takes place right after scan j has started. When using logarithmic intensities, the model becomes linear in α and κ :

$$J_i(t_{ij}) = J_i^0 - \alpha t_{ij} - (j - 1)\kappa. \quad (3.14)$$

As before, it is assumed that the log-intensities for all mice at $t = 0$ follow a normal distribution, $J_i^0 \sim \mathcal{N}(\mathcal{J}, \sigma_{\mathcal{J}}^2)$, and similarly for the measurement error term, except for the addition of an index j designating the scan number of each sample, $\epsilon_{ij} \sim \mathcal{N}(0, \sigma^2)$. The stochastic variables are then given as follows:

$$\tilde{J}_{ij} = J_i(t_{ij}) + \epsilon_{ij}, \quad (3.15)$$

$$\epsilon_{ij} = \tilde{J}_{ij} - J_i(t_{ij}) = \tilde{J}_{ij} - J_i^0 + \alpha t_{ij} + (j - 1)\kappa. \quad (3.16)$$

We again assume that the stochastic variables, J_i^0 and ϵ_{ij} , are independent which lets us express the joint PDF as product of each PDF for J_i^0 for $i = 1, \dots, n$ and ϵ_{ij} for $i = 1, \dots, n$ and $j = 1, \dots, \mu(i)$. We will ignore the normalization constant of each PDF as this does not change the solution to the optimization problem. The likelihood function in this case becomes:

$$\begin{aligned} \mathcal{L} &= \prod_{i=1}^n \left[\text{PDF}(J_i^0) \cdot \prod_{j=1}^{\mu(i)} \text{PDF}(\epsilon_{ij}) \right] \\ &= \prod_{i=1}^n \left[\exp\left(-\frac{(J_i^0 - \mathcal{J})^2}{2\sigma_{\mathcal{J}}^2}\right) \cdot \prod_{j=1}^{\mu(i)} \exp\left(-\frac{(\tilde{J}_{ij} - (J_i^0 - \alpha t_{ij} - (j - 1)\kappa))^2}{2\sigma^2}\right) \right], \end{aligned} \quad (3.17)$$

where the second equality sign is understood to mean ‘‘equal up to multiplication by a positive constant’’. Applying the negative logarithm gives:

$$-\log \mathcal{L} = \frac{1}{2} \sum_{i=1}^n \left[\frac{(J_i^0 - \mathcal{J})^2}{\sigma_{\mathcal{J}}^2} + \sum_{j=1}^{\mu(i)} \frac{(\tilde{J}_{ij} - (J_i^0 - \alpha t_{ij} - (j - 1)\kappa))^2}{\sigma^2} \right], \quad (3.18)$$

and the minimization problem becomes:

$$\hat{\boldsymbol{\theta}} = \arg \min_{\boldsymbol{\theta}} \left[\frac{1}{2} \sum_{i=1}^n \rho^2 (J_i^0 - \mathcal{J})^2 + \frac{1}{2} \sum_{i=1}^n \sum_{j=1}^{\mu(i)} (\tilde{J}_{ij} - (J_i^0 - \alpha t_{ij} - (j - 1)\kappa))^2 \right], \quad (3.19)$$

where $\boldsymbol{\theta} = [J_1^0, \dots, J_n^0, \mathcal{J}, \alpha, \kappa]$. Given measured intensities and corresponding times, $\{(t_{ij}, \tilde{J}_{ij})\}$, and a value for ρ^2 , we can solve this minimization problem in the manner discussed in the previous section. This yields parameter estimates $\hat{\boldsymbol{\theta}}$ in the model that takes both chemical degradation and photobleaching into account.

3.3 Casting the Model as a Mixed-effects Model

While we have derived the model and estimators from first principles, the model fits into the framework of linear mixed-effects models. Indeed, for each i, j

$$\tilde{J}_{ij} = \mathcal{J} + u_i - \alpha t_{ij} - (j - 1)\kappa + \epsilon_{ij},$$

where we have written $J_i^0 = \mathcal{J} + u_i$. So the model depends both linearly on the vector of fixed effects $\beta = (\mathcal{J}, \alpha, \kappa)$, and random effects $\mathbf{u} = (u_1, \dots, u_n)$. In particular, there exists matrices \mathbf{X} and \mathbf{Z} so the model is written

$$\tilde{\mathbf{J}} = \mathbf{X}\beta + \mathbf{Z}\mathbf{u} + \epsilon.$$

In practical terms, R and Python libraries can be used for estimating the parameters, and the properties of the estimators are well understood, see e.g. [4].

3.4 Generation of Synthetic Data

Since data set 1 does not contain enough data points for a reliable estimation, and the samples lack a history of both chemical degradation and photobleaching, we instead test the method proposed in the previous section using a synthetic data set. The artificial data are generated using the assumptions stated in Section 3.1, and the parameters in the model are held fixed.

We generate 2000 independent subjects, each with its own initial intensity drawn from a log-normal distribution, such that the log-intensities are normally distributed. For subject i , we then simulate k_i measurements, with k_i being discrete and i.i.d. stochastic variables between 1 and 5 with uniform probability. The time between measurements for a single subject is exponentially distributed, with a mean of 15 days between measurements. When measuring at time t' , the model is applied along with the chosen parameters to get the current intensity of subject i at time t' based on the previous intensity.

Measurement noise is multiplied onto the values before the values are saved. After a value has been saved, the photobleaching effect is simulated by multiplying the intensity with a constant factor. To summarize, we perform the following steps for each subject:

- (1) Initialize an intensity value by sampling from a log-normal distribution.
- (2) Randomly decide number of scans to perform on the subject ($1 \leq k_i \leq 5$).
- (3) Sample time point of next imaging event, $t_{\text{next event}}$.
- (4) Forward time to next event and scale intensity value by $e^{-\alpha\Delta t}$,
where $\Delta t = t_{\text{next event}} - t_{\text{now}}$.
- (5) Apply measurement noise to the intensity value and save it⁴.
- (6) Apply photobleaching by multiplying with known constant.
- (7) If another image is taken, repeat from (3).

⁴ The measurement noise only affects the saved values and hence does not affect later measurements.

Table 2. Estimated parameters where $\rho^2 = 0.01$. Groups 2 and 6 contain only five observations each.

Group	$\hat{\alpha}$	$\hat{\mathcal{J}}$	\hat{J}_1^0	\hat{J}_2^0	\hat{J}_3^0	\hat{J}_4^0	\hat{J}_5^0	\hat{J}_6^0
1	0.0076	5.3721	5.3913	5.4270	5.3719	5.3783	5.3498	5.3144
2	0.0400	9.8139	9.2198	10.3299	10.2738	10.0215	9.2245	NA
3	0.0500	8.9859	8.9673	9.3040	10.1789	9.2171	7.7028	8.5453
4	0.0562	8.2881	8.3320	7.9539	8.4539	8.1021	8.0109	8.8758
5	0.0014	8.2317	9.0082	7.8910	6.5811	8.2911	8.9944	8.6242
6	0.0352	8.7075	8.6780	8.8225	9.2974	8.5840	8.1554	NA

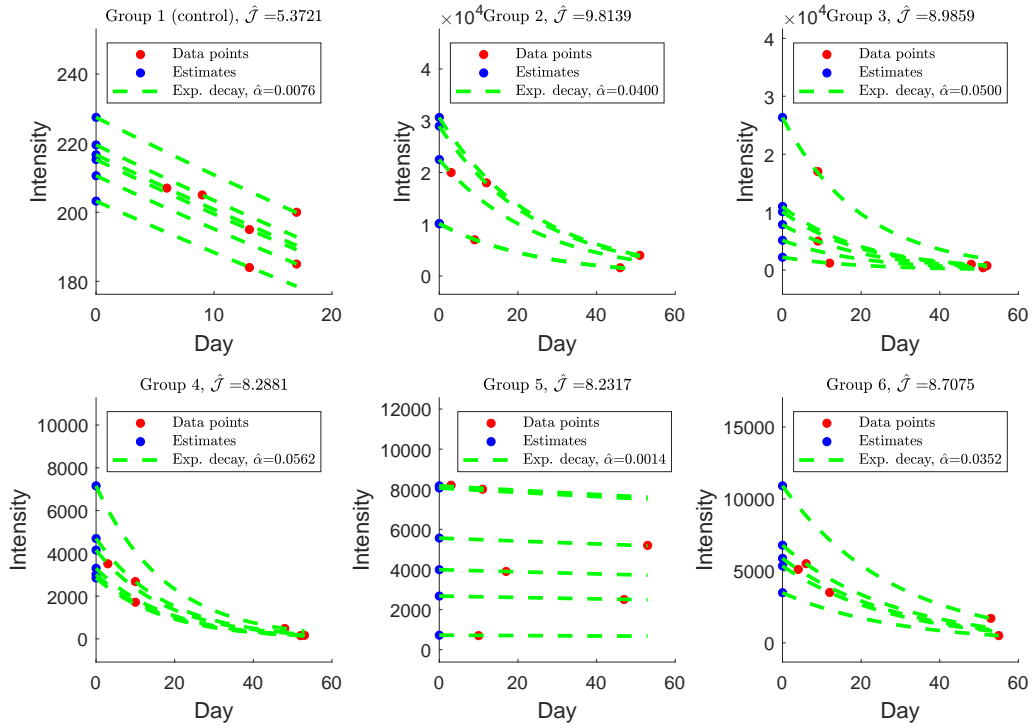


Figure 4. Intensity vs. time modelled using maximum likelihood estimates $\hat{\alpha}$, $\hat{\mathcal{J}}$ and \hat{J}_i^0 listed in Table 2. Measured values ($\tilde{I}_i = \exp(\tilde{J}_i)$) and estimated initial values ($\hat{I}_i^0 = \exp(\hat{J}_i^0)$) are shown as red resp. blue points.

4 Results

4.1 Chemical Degradation

We perform the optimization using Equation (3.12) with the fluorescent specific data for the six different groups using MATLAB's `fmincon` function with an interior-point algorithm. Results acquired for $\rho^2 = 0.01$ are summarized in Table 2, and the corresponding plots of intensity vs. time are shown in Figure 4.

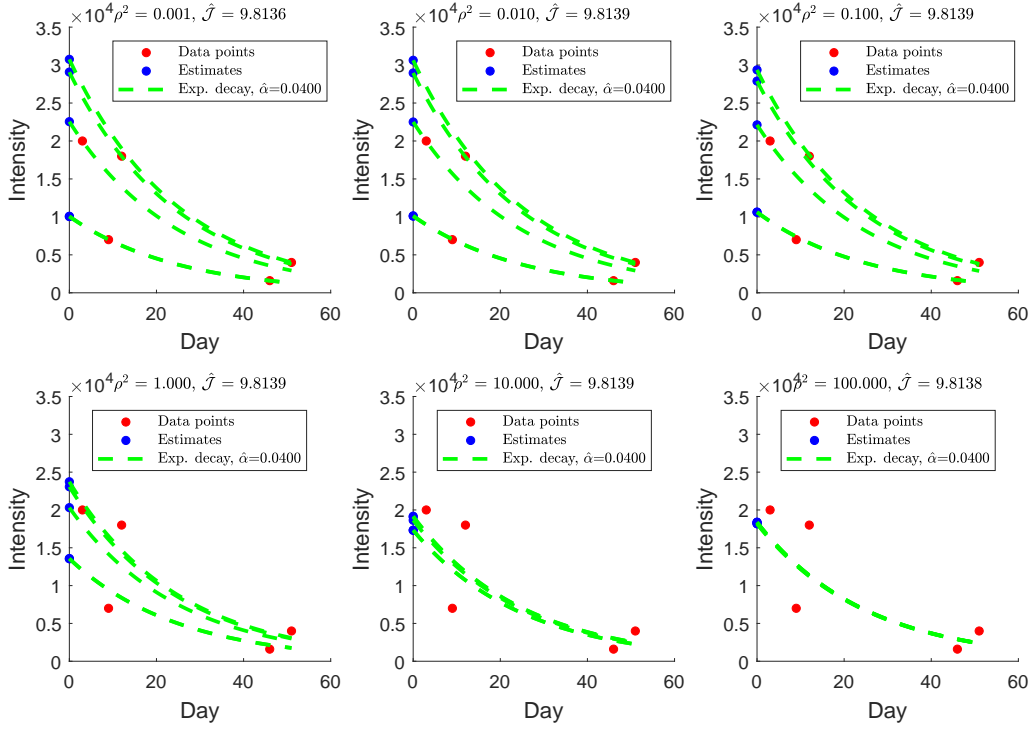


Figure 5. Similar to Figure 4, plots showing Group 2 and varying values of ρ^2 .

The sensitivity of results on the choice of ρ^2 is examined by repeating this analysis for Group 2 with different values of ρ^2 . The results are shown in Figure 5. We note that the estimates $\hat{\alpha}$ and \hat{J} seem to be very robust against variations in ρ .

The estimation of the initial intensity of each mouse enables the correction and comparison of samples with different histories as seen in Figure 6, where the observed intensity is compared with the corrected intensity, i.e. the estimated initial intensity. This has been done for each individual mouse in each group. We observe that the corrections made appear reasonable, and that the corrected intensities generally tend to be of larger magnitude than the observed intensities, as one would expect due to the degradation. However, the standard deviation of the observed intensities (at multiple different times) and the standard deviation of the predicted intensities at time $t = 0$ is roughly the same in all cases. Thus, our corrections have not reduced the standard deviation of the samples (see the discussion in Section 5.2). Lastly, it is seen from group 1 (the control group) that there is no significant difference between the corrected intensities and the observed intensities, while there seems to be a distinct difference for the other groups (except group 5), as desired. The exception of group 5 is likely due to the specific compound used for this group.

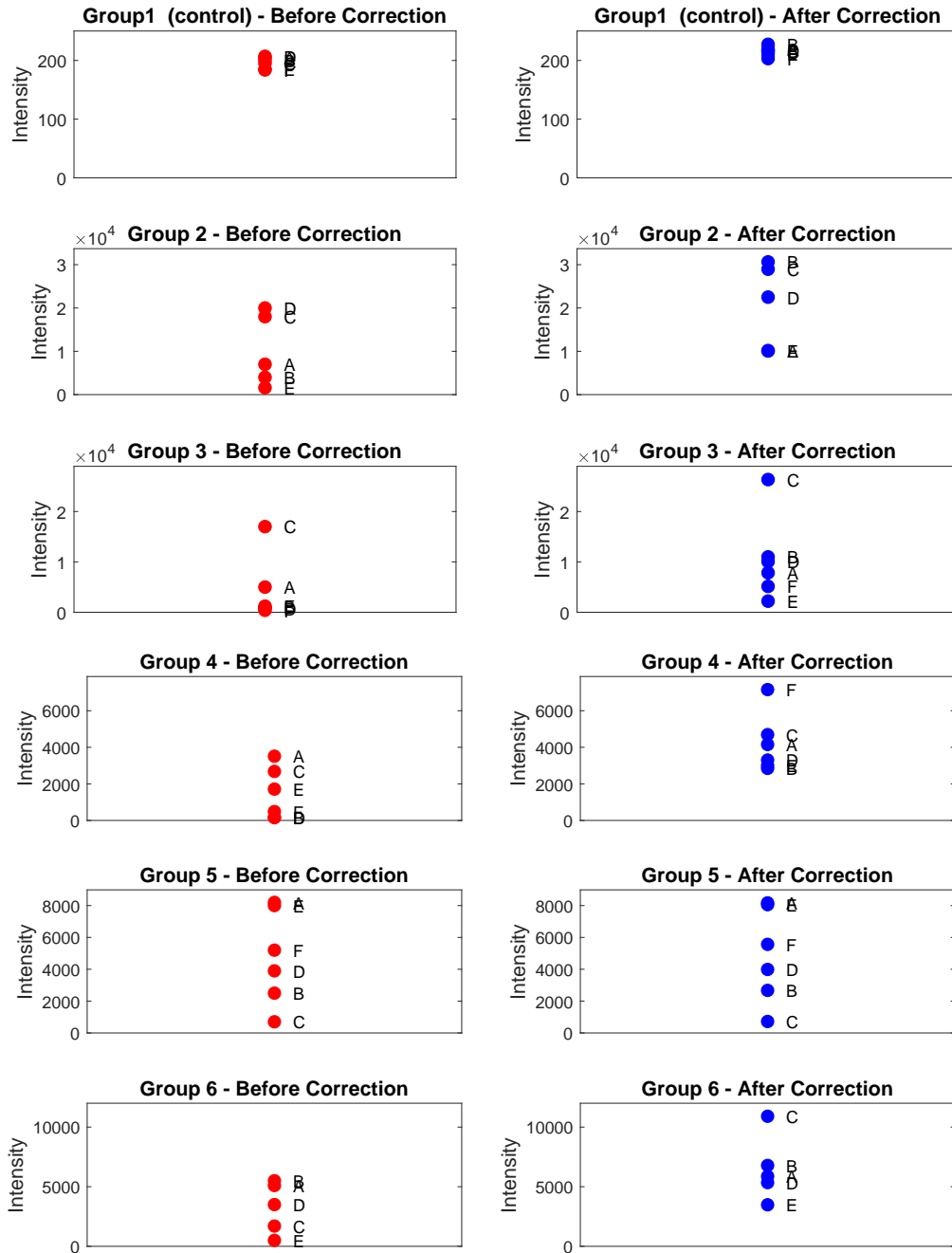


Figure 6. A comparison of the intensity of each mouse in group 1-6 before (left) and after corrections (right). The corrections are acquired by estimating the initial intensity of each mouse with the proposed model.

Table 3. Best fit parameters and residual spread for photobleaching data using the model in Equation (4.1).

Chemical Compound	$\hat{\kappa}$	\hat{c}	\hat{b}	σ_{resid}
Lectin	$7.227 \cdot 10^{-3}$	3170.1	2403.4	86.4
Cy5	$1.536 \cdot 10^{-2}$	4153.8	3426.6	161.6

4.2 Photobleaching

In data set 2, the time span between the first and last data point is very small compared to data set 1, so we can neglect chemical degradation. We therefore fitted the data with the model

$$I(n) = c \cdot e^{-\kappa n} + b, \quad (4.1)$$

i.e., an exponential decay with constant background intensity, as shown in Figure 7. The inclusion of a constant background intensity as an extra parameter was found to dramatically improve the fit compared to the model with no background. The fitting parameters yielding the best fits using the model with background are summarized in Table 3, along with the residual spreads.

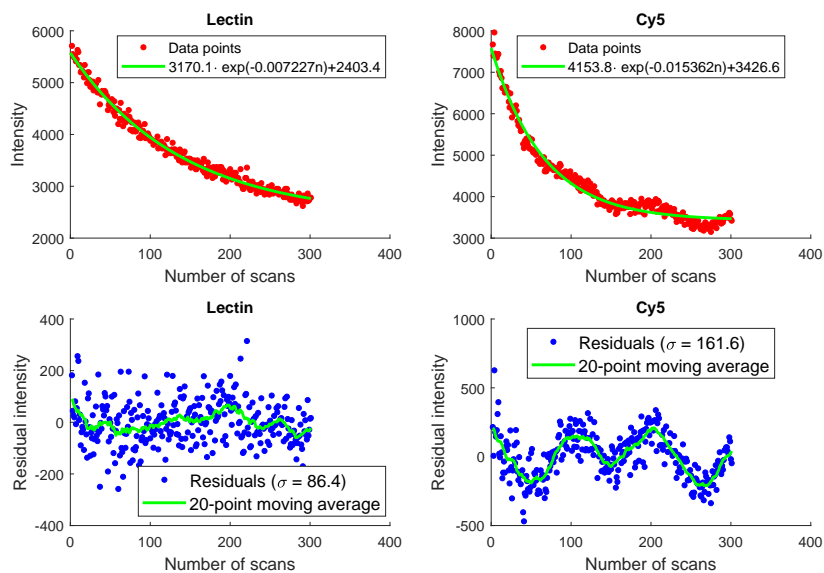


Figure 7. Top row: data set 2, measured intensity vs. number of scans (dots), and best fit (lines) using the model given in Equation (4.1) for the fluorophores Lectin (left) and Cy5 (right). Bottom row: residuals and their 20-point moving averages.

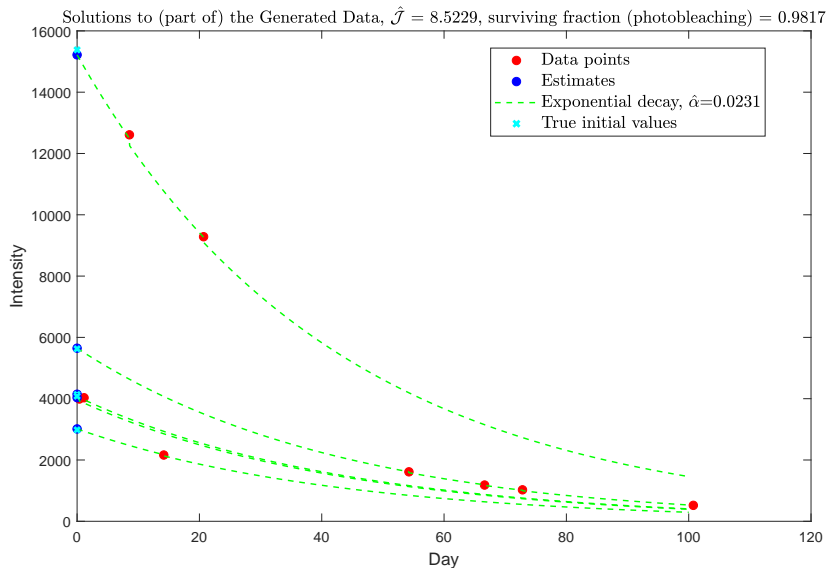


Figure 8. Intensity vs. time modelled using maximum likelihood estimates $\hat{\alpha}$, \hat{J} and \hat{J}_i^0 for the first 5 mice of the artificially generated data set. Synthesized measurement values ($\tilde{I}_i = \exp(\tilde{J}_i)$) and estimated initial values ($\hat{I}_i^0 = \exp(\hat{J}_i^0)$) are shown as red resp. blue points. The true synthesized initial values are shown as cyan crosses.

4.3 Artificially Generated Data

We have also applied Equation (3.19) to the artificially generated data. The results of (some of) this optimization can be seen in Figure 8. From this figure, we notice that the predicted initial values lie very close to the true generated initial values. This is true not only for the first 5 mice but for all 2000 mice in the data set. The average relative deviation between the true generated initial values and the estimated initial values, i.e. the difference between the true I_i^0 s and the estimated \hat{I}_i^0 s, is 0.3907%, and the largest relative deviation is 2.4933%.

5 Discussion

5.1 Discussion of Assumptions

The model contains multiple assumptions (see Section 3.1) worth discussing. Firstly, we assume that the chemical degradation can be described by an exponential decay in the intensity. This corresponds to a first order decay of the fluorescent labels and is one of the simplest possible reactions we can imagine. The experiments performed in [1] also suggest that the fluorescence decay over time can be modelled as a first order exponential. One could consider using a more complex reaction type assumption, but to justify this one would need more data. With the currently available data, we cannot say much about the reaction type, and have for this reason chosen this very simple model for intensity decay.

The second assumption of the model is that only a fixed fraction of the fluorescent

label survives each scan due to photobleaching. This is another simplifying assumption. In reality, the effect of photobleaching is far more complex than simply removing a set fraction of the molecules. It could e.g. be a single-exponential decay or even more complex than this [2]. However, as the samples are only scanned for a few seconds and typically only 1, 2 or 3 times⁵ during a storage period lasting from several days to a few weeks, the total time of photobleaching of each sample is very small compared to the time scale of chemical degradation. Thus, we can approximate the behavior of the fluorescent labels in these short time intervals of photobleaching by simply removing a set fraction of the intensity.

The third assumption of the model is that the intensity obtained in a scan depends only on the amount of labeled compound remaining at the start of the scan. Thus, no other compounds, lighting or other effects contribute to the measured intensities. This is once again a simplifying assumption, as some effects might influence the measurements in reality. However, if the measurements are made in a controlled environment, we expect these effects to be quite small, and therefore the assumption might hold to a large extent.

Additionally, we assume that the log-intensities for all mice at $t = 0$ follow a normal distribution with mean \mathcal{J} and variance $\sigma_{\mathcal{J}}^2$, i.e., $J_i^0 \sim \mathcal{N}(\mathcal{J}, \sigma_{\mathcal{J}}^2)$, and that the log-measurement errors also follow a normal distribution, this time with mean zero and variance σ^2 , i.e., $\epsilon_i \sim \mathcal{N}(0, \sigma^2)$. These assumptions are very practical as they lead to simpler equations when finding the maximum likelihood estimates of the parameters, compared to other possible distributions. Once again the data is very limited, and it is therefore very difficult to test if these assumptions are reasonable. For example, we have no data for the mice at day 0, and thus we cannot know whether the assumption on the initial log-intensities is reasonable. To assess this assumption, we need more data.

However, we can discuss the assumption on the measurement error. We expect the microscope to measure the correct value *on average*, though the measured values of course vary on each measurement. We also assume that the variance of the measurement errors is constant. Though this is a very convenient assumption, it is probably not correct. As the fluorophores decay, measuring intensities accurately becomes more difficult, and information is lost as intensities decay below the sensitivity threshold of the microscope. Thus, the measurement errors increase over time. This could be incorporated into the model (see Section 6), but we have not had the time to do so.

5.2 Discussion of Results

5.2.1 Biological variance and measurement variance

We find that estimates of initial intensities J_i^0 depend strongly on the parameter ρ^2 , whereas the chemical decay rate α is rather robust against variations in ρ^2 . This is to be expected; when ρ^2 is increased, we force the values of J_i^0 to have less variance in the optimization problem in Equation (3.12), and vice versa.

While an estimate for ρ^2 could be made given data that allowed for estimates of both σ^2 and $\sigma_{\mathcal{J}}^2$, all we can do with the data available to us is to describe the behavior of the solutions acquired by the model for different values of ρ^2 . As $\rho^2 \rightarrow \infty$, $\sigma_{\mathcal{J}}^2$ becomes

⁵ Casper G. Salinas, Gubra; private communication.

smaller compared to σ^2 . This corresponds to the extreme case where “all mice are created equal”, i.e., there is no biological variation, and all mice have exactly the same intensity at time $t = 0$ (and thus also at all later times). In this case, all variance observed in measured intensities can be ascribed to the measurement error. The other extreme case is $\rho^2 \rightarrow 0$, where $\sigma_{\mathcal{J}}^2$ becomes much larger than σ^2 . This is the case when there is no or very little uncertainty associated with measurements, and all variance in measurements can be ascribed to biological variance.

The truth lies somewhere between these two extremes; the problem is finding out where. σ^2 is likely easier to estimate than $\sigma_{\mathcal{J}}^2$. For instance, as mentioned, in data set 2 we neglect chemical degradation and we can easily correct for photobleaching. There is also no biological variance since data points from this series of repeated scans come from the same sample. Sensor noise therefore dominates the remaining variation in the data, and the variance of the residuals of the model given by Equation (4.1) in data set 2 (cf. Table 3) might be a first step towards estimates of σ^2 . This approach presupposes that the residuals are dominated by noise, or equivalently, that the model with which the data are fitted accurately captures the relevant dynamics.

The residual plots in Figure 7 suggest that the exponential decay with constant background models the data set for Lectin very well, as the residuals are small and randomly distributed. Larger residuals displaying a non-random distribution with clear undulations are found for Cy5, implying that there is an additional effect apart from the exponential decay in the model. Deviations from the model appear to oscillate with a period of about 100 scans, corresponding to about 10 minutes. While we do not have a definite explanation for this, it is possible that the scanning conditions (duration, temperature, laser intensity, etc.) shifted during the recording of this data set to produce a non-constant decay rate, or some (possibly periodic) external error source may have been at play.

These observations suggest that σ^2 can be reliably estimated for Lectin based on the data available, whereas estimates of σ^2 for Cy5 would be more questionable. Estimating $\sigma_{\mathcal{J}}^2$ is more difficult. To do this, we would need measurements of many samples on day 0 with the only source of variation being the samples coming from different mice. Determining ρ^2 requires both σ^2 and $\sigma_{\mathcal{J}}^2$ to be known (or estimated), which is not possible based on the available data. Indeed, this would require a batch where there are multiple samples and where at least one sample is scanned more than once. However, in data set 1, each batch was scanned only once, and in data set 2, there was only one sample (for each fluorophore).

Overall, we would expect the biological variance to be much larger than the variance of the measurement errors. Thus, unless otherwise noted, we have used a value of $\rho^2 = 0.01$ in this report.

5.2.2 Initial intensity estimates

Inspecting Figure 6, we see that we were able to reorder the observed intensities into the order of the predicted intensities at time $t = 0$. We note that with our choice of $\rho^2 = 0.01$, the standard deviation of the observed intensities (at multiple different times) and the standard deviation of the predicted intensities at time $t = 0$ is roughly the same in all cases. This should not be interpreted to mean that the initial intensities given by the

model are not more accurate than using the measured intensities directly. Using a small value of ρ^2 means assuming that the biological variance is large compared to variance due to measurement errors. In the case of data set 1, this turns out to mean that the model predicts that the variance in the data is due to biological variance. Since biological degradation and photobleaching both lower fluorescence, using the measured intensities as estimators of initial intensities would systematically underestimate intensity, and these estimators would therefore be biased. The estimators given by the model do not significantly reduce the variance (as it is ascribed to biological variance), but should remove the bias. The benefit of the estimates (in the particular case of data set 1, with ρ quite small) thus lies in removing bias, not in reducing variance.

As previously discussed, ρ^2 determines the standard deviation and variance of our estimates of the initial intensities. Therefore, the reduction in variance between the observed intensities and the predicted intensities at time $t = 0$ depends crucially on the value of ρ^2 . A larger value of ρ^2 will lead to a greater reduction in variance, and vice versa.

As previously discussed, the assumption that the measurement errors on the logarithmic scale are of the same variance, independent of time, is quite dubious. When the fluorescence from the label has low intensity, ambient fluorescence may drown out the signal, causing the relative measurement uncertainty to increase with time. Thus, a more realistic assumption would be that measurement errors are on the same order of magnitude on the absolute scale. We can correct for this by making the variance of the measurement errors larger with time, which would mean that earlier data points a given greater weight than the later data points. We have not had the time to implement this at this point. Additionally, we can likely get better results by having access to more data and better estimates of the parameters in the model.

5.2.3 Synthetic data

The results obtained from applying the model to the synthetic data (see Section 4) are likely to be overly optimistic. The generated data behaves *exactly* as we assume in the model, and thus the model *ought to* give a good fit to the data. Thus, testing the model on the artificially generated data does not tell us if the model actually works on real data, but it does act as a sanity check, showing that the model works if the data behaves as we assume.

5.2.4 Impact of photobleaching

The estimation of the decay of the fluorescent labels due to photobleaching shows that only a very small percentage of the intensity is lost at each scan for the two chemicals Lectin and Cy5. Since each sample is only scanned a few times in practice, the overall effect of photobleaching is minor for both Lectin and Cy5. If the same is true for other fluorescent labels, the effect of photobleaching might be negligible. However, we once again need more data and testing to state this with certainty.

6 Future Work

Assuming that the signal on a given pixel in a picture (e.g. from a microscope) is not fully extinguished by degradation, and neglecting the quantization effects, an estimate of its original intensity should be possible to do well by reversing the scaling. However, to improve the estimates, we would need more data. Ideal data should be similar to the synthetic data where many subjects have been measured several times such that both the chemical degradation and photobleaching parameters can be estimated. This would then allow for also testing the model assumptions, and if they are incorrect or lacking, a new model could be proposed.

Additionally, it would make sense to estimate the influence of the measurement error vs. the biological variance in an isolated manner. To estimate the variance σ^2 of the sensor, a data set like data set 2, but with more subjects and more chemical compounds, would be helpful. As for the biological variation, $\sigma_{\mathcal{J}}^2$, between the mice, this could best be estimated with a large number of measurements of the intensity at day 0 with different subjects injected the same compound. This would allow a better estimate of ρ^2 .

The objects, being photographs, represent real objects, and therefore there is a correlation with respect to the intensity value in neighbouring pixels. Assuming data is not an issue, it would then be possible to design a neural network which, given an image of a sample that has degraded and been affected by photobleaching, could recreate how the images would have looked on day 0. Work by Gao *et al.* demonstrates a neural network which restores vintage photographs [3].

This would require images of the relevant tissue at day 0 and at various later points for several subjects. It would here be important that the images are aligned such that a pixel in an image from day 0 corresponds to the same point in the tissue in later images of that subject.

Both the chemical degradation and the photobleaching will, as time progresses, end up degrading the fluorescence label to a degree where it will not be possible to distinguish the intensity of the fluorescence from the background. This means that the model will tend to undershoot as time progresses, hence have intensity values of smaller magnitude than of what is actually the case. We therefore propose that a more sophisticated model be developed which takes this into account, for instance by introducing a weight term.

For the models presented in this report one should also investigate how certain the parameter estimates are, quantifying how much we would expect the parameters estimated using the new data to deviate from the parameters estimated using the original data, given that the experiment in its entirety was repeated. Depending on the model, one may do this using bootstrapping.

7 Conclusion

From the above conducted analysis and results, we conclude that the developed models enabled the estimation of the initial intensity value of each fluorescent label for each mouse.

Due to the nature of data available to us, we could not estimate the value of ρ^2 . It is necessary to have an idea of ρ^2 to estimate the initial intensity values. We observed

that the value of ρ^2 had a large influence on the individual estimated initial intensity values, J_i^0 , but a much smaller effect on the estimate of the expected initial intensity of the sample, \mathcal{J} , and decay rate, α .

Furthermore, we conclude that the effect of the photobleaching may be negligible as its effect upon the degradation of the fluorescence is minor.

All in all, we have found and applied a model that takes into account both the chemical degradation of the fluorescent labels as well as the degradation due to photobleaching, thus permitting the correction and comparison of samples with different histories.

Acknowledgements

We would like to express our gratitude to Casper G. Salinas from Gubra for helping us continuously throughout the extent of the project by providing meaningful discussion, insights and data.

References

- [1] Shahnaz M. Quadri Abeer A. Alnuami, Buthaina Zeedi and S. Salman Ashraf. Oxyradical-induced gfp damage and loss of fluorescence. *International Journal of Biological Macromolecules*, 43:182–186, 2008.
- [2] I. Ted Young E. J. Hennink and Hans J. Tanke. Photobleaching kinetics of fluorescein in quantitative fluorescence microscopy. *Biophysical Journal*, 68:2588–2600, 1995.
- [3] Qifan Gao, Xiao Shu, and Xiaolin Wu. Deep restoration of vintage photographs from scanned halftone prints. *Proceedings of the Ieee International Conference on Computer Vision*, 2019-:4119–4128, 2019.
- [4] G. K. Robinson. That blup is a good thing: The estimation of random effects. *Statistical Science*, 6(1):15–32, 1991.